Update on External Kink Calculations

NIMROD Team Meeting 2016 — Sherwood

K.J. Bunkers & C.R. Sovinec

University of Wisconsin-Madison

◊ External kinks are important for disruption processes, including vertical displacement events.

- External kinks are often associated with Vertical Displacement Events (VDEs).
  - VDEs can cause large vertical ($\sim 150\,\mathrm{MN}$) and horizontal forces ($\sim 50\,\mathrm{MN}$) on the confinement vessel[1]. These are among the largest disruption forces.
  - The physical movement of the plasma into the wall causes large heat loads.
- Computations can help quantify the safety margins needed for VDEs[2,3,4]
  - The vertical and horizontal forces on the device can be calculated.
  - Heat loads can be assessed.
  - Currents in the device can be calculated.
  - One can predict the onset of 3D instability and its effects.

[1] ITER Physics Basis 1999

[2] Strauss, Paccagnella, and Breslau, Phys. Plasmas **17**, 082505 (2010)

[3] Paccagnella, Strauss, and Breslau, Nucl. Fus. **49**, 035003 (2009)

[4] Zakharov, Phys. Plasmas **15**, 062507 (2008)

External kinks are challenging, but important phenomena to study computationally.

- External kinks can cause strong non-axisymmetric distortions of the plasma. This requires a large number of Fourier components to resolve in NIMROD.
- If there is sharp variation in the toroidal direction, an accurate Fourier representation can be difficult. For example, temperature values can go negative, creating ill-conditioned matrices.

◊ We apply extended, nonlinear, non-ideal MHD modeling to describe plasma evolution.

$$\frac{\partial n}{\partial t} + \boldsymbol{\nabla} \cdot (n\mathbf{V}) = \boldsymbol{\nabla} \cdot (D_n \nabla n - D_h \nabla \nabla^2 n)$$

Continuity with diffusive numerical fluxes

$$mn\left(\frac{\partial}{\partial t} + \mathbf{V} \cdot \nabla\right)\mathbf{V} = \mathbf{J} \times \mathbf{B} - 2\nabla(nT) - \boldsymbol{\nabla} \cdot \overleftrightarrow{\boldsymbol{\Pi}}$$

flow evolution

$$\frac{3}{2}n\left(\frac{\partial}{\partial t} + \mathbf{V} \cdot \nabla\right)T = -nT\boldsymbol{\nabla} \cdot \mathbf{V} - \boldsymbol{\nabla} \cdot \mathbf{q}$$

temperature evolution

$$\frac{\partial \mathbf{B}}{\partial t} = -\boldsymbol{\nabla} \times (\eta \mathbf{J} - \mathbf{V} \times \mathbf{B}) + \kappa_{\mathrm{B}} \nabla \boldsymbol{\nabla} \cdot \mathbf{B}$$

Faraday's/Ohm's Law with numerical error control

$$\mu_0 \mathbf{J} = \boldsymbol{\nabla} \times \mathbf{B}$$

low-ω Ampere's law

$$\overleftrightarrow{\boldsymbol{\Pi}} = -\rho\nu\overleftrightarrow{\mathbf{W}}, \quad \overleftrightarrow{\mathbf{W}} = \nabla\mathbf{V} + (\nabla\mathbf{V})^{\mathsf{T}} - \frac{2}{3}\boldsymbol{\nabla} \cdot \mathbf{V}$$

◊ We examine external kinks in a simple configuration.

- External kinks occur during VDEs when plasma interacts with the surface, scraping off the edge region.
- The unstable modes are resonant ($q = m/n$) outside the plasma.
- Nonlinear cylindrical simulation results show the shape of the distortion late in time ($t = 870\tau_A$) for a large aspect ratio cylinder ($R/a = 10$) $(m, n) = (2, 1)$ kink.

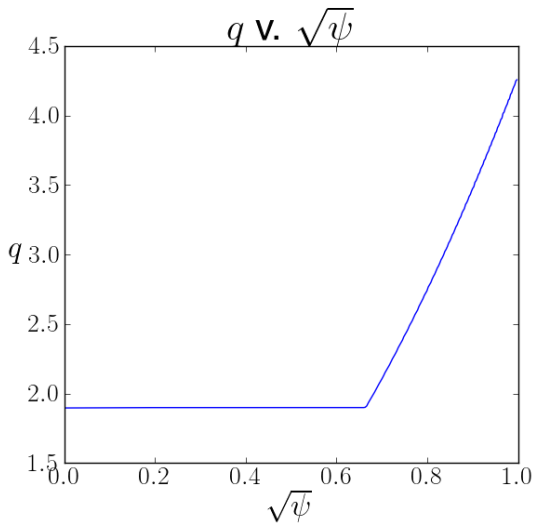

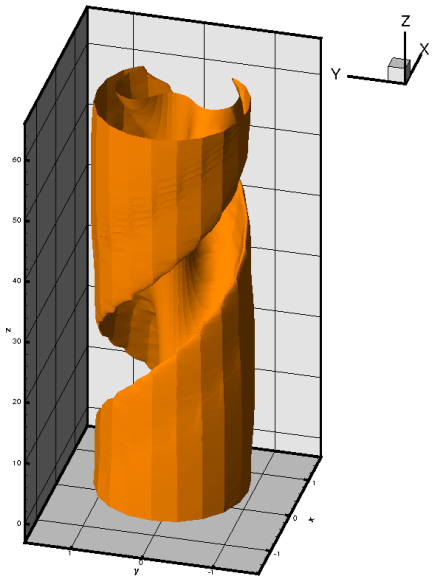

It is important to distinguish the plasma surface in the numerical representation.

- Having too few Fourier components in the simulation leads to Gibbs-like phenomena that causes the simulation to crash.
- When the number of Fourier components increases, the simulation can be run longer, and the Gibbs phenomenon is less severe.
- We can see the instability looks like a vacuum bubble[5].

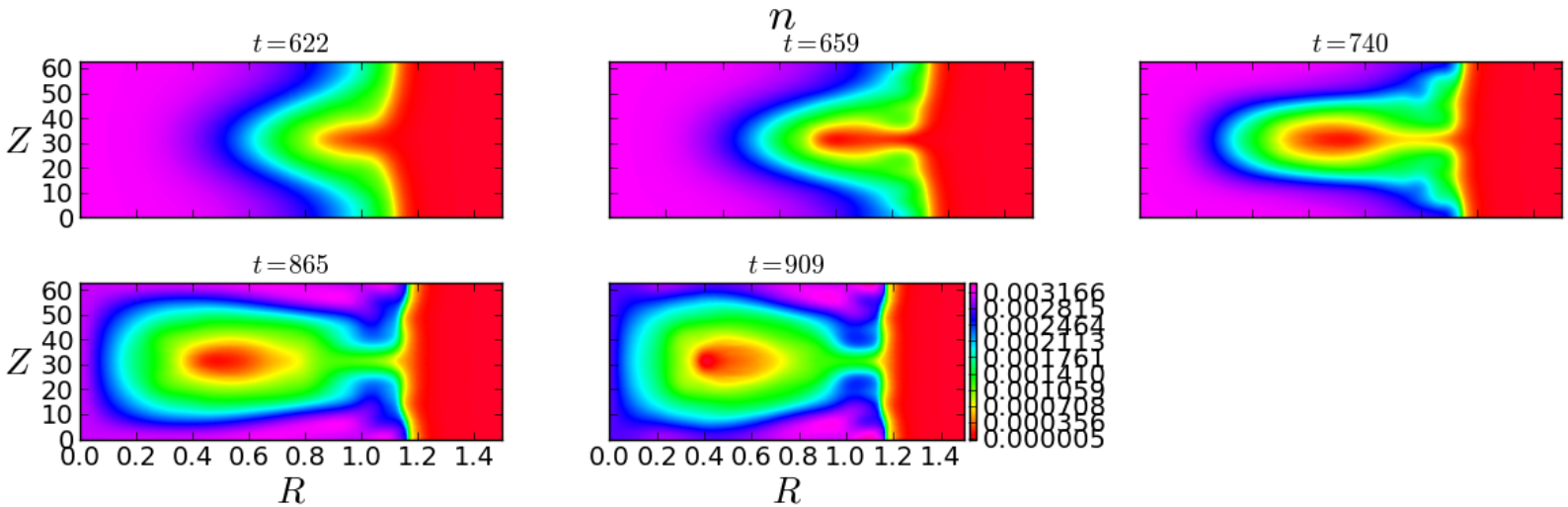

[5] Rosenbluth, Monticello, Strauss and White, Phys. Fluids **19** (1976)

A nonlinear computation with the same equilibrium demonstrates external kink distortion in toroidal geometry.

- Resistivity is determined by the evolving 3D temperature distribution.
- (2,2) and (3,3) components are large in this case.

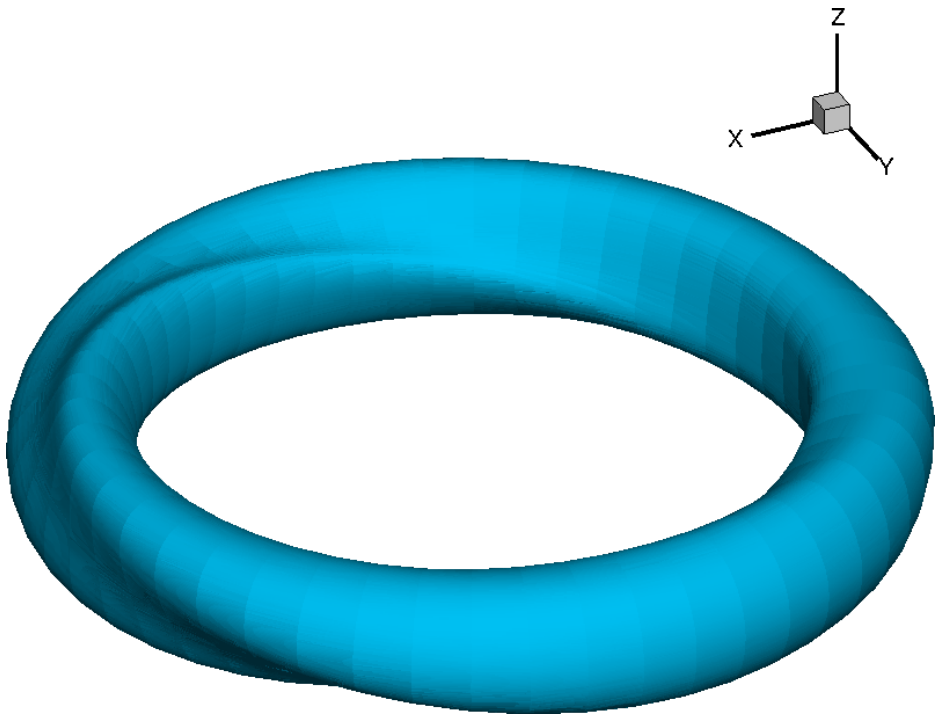

Surface of constant pressure at $p(0)/8$ shows the plasma shape.

The (1,1) external kink has also been simulated and shown similar behavior.

- Nonlinear cylindrical simulation results show a similar distortion for a $(1, 1)$ kink at $t = 450\tau_A$.
- $(1, 1)$ kinks have proven to be more difficult to simulate. They have smaller time steps than the $(2, 1)$ kinks. In addition, more Fourier components are needed.

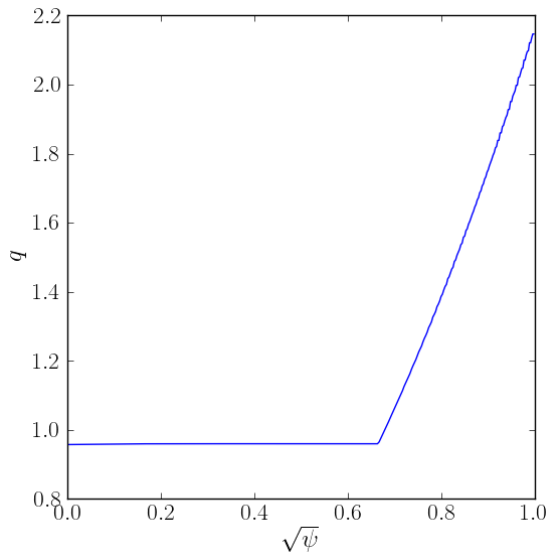

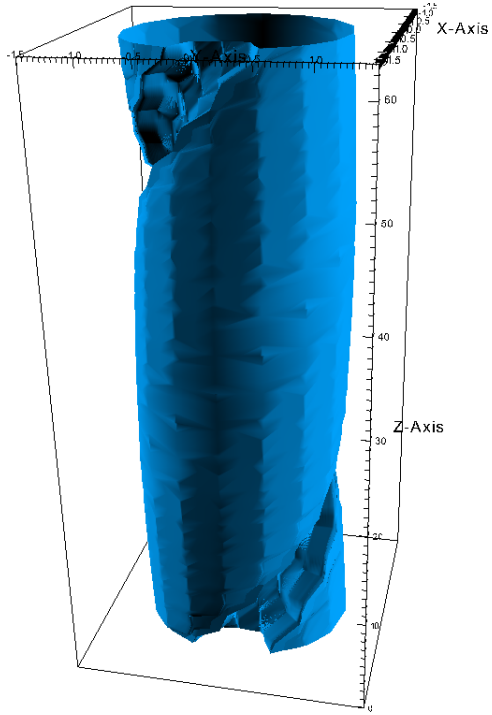

◊ NIMROD uses Fourier components in the toroidal direction.

- In NIMROD, quantities in the toroidal direction are calculated using a Fourier decomposition. For quantity b we write

$$b(\varphi_j) = b_0 + \sum_{n=1}^{N_D-1} \left(b_n e^{in\phi_j} + \text{c.c.} \right)$$

$$\phi_j = \frac{2\pi}{N} j\,, \quad j = 0, 1, \ldots, N-1$$

with N_D the number of Fourier components to keep for dealiasing, and N the total number of Fourier components.

A Fourier transform with dealiasing is used to prevent aliasing error.

- Dealiasing removes some of the high-frequency components to prevent what the high frequencies from being sampled on the grid as lower frequencies.
- This is controlled by using $N_D = \text{floor}(N/3) + 1$ in `NIMROD`.
- For a function with small scales, dealiasing can enhance overshoot, possibly leading to negative values for quantities that must be non-negative (such as temperature or resistivity).
- One proposed method to reduce overshoot error is to use least squares with the data from the toroidal grid.

Strong toroidal variation creates computational challenges.

- For external kinks, $\eta(\varphi)$ has relatively sharp jumps.
- Below the original and dealiased inverse Fourier transform for some quantity T. (2^{ℓ_φ} is the number of grid points.)

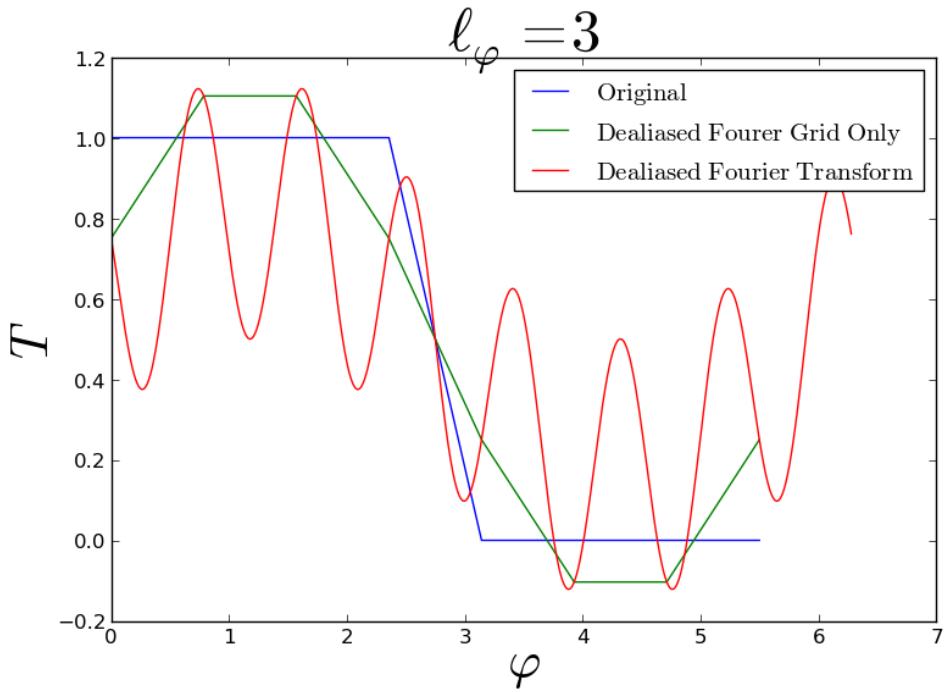

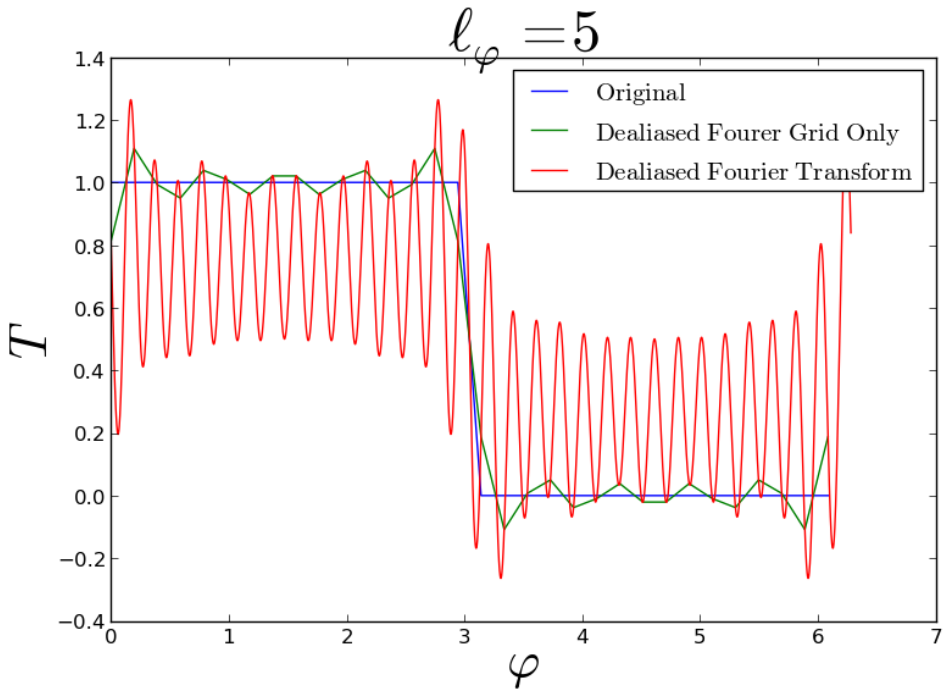

For test problem, the least squares method leads to some improvement, but not drastically improved.

- We compare the pure dealiased method with the least squares Fourier method and find very little difference.
- The plot below includes taking data from linearly interpolating between known toroidal points on the grid (5 points between each original grid point here). When no interpolated data is used, the dealiased and least squares (LSQ) results coincide.

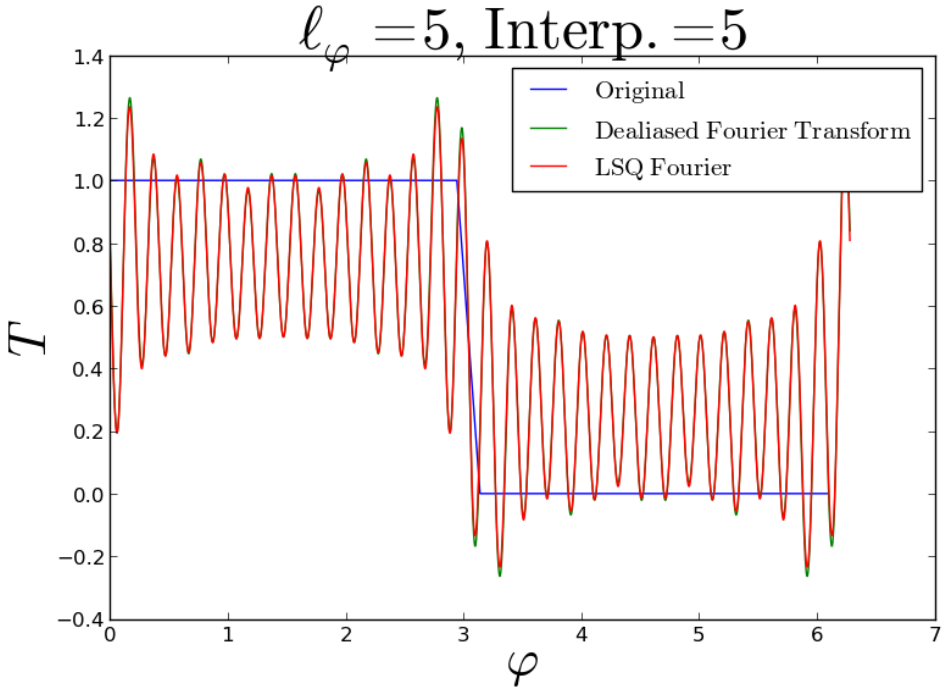

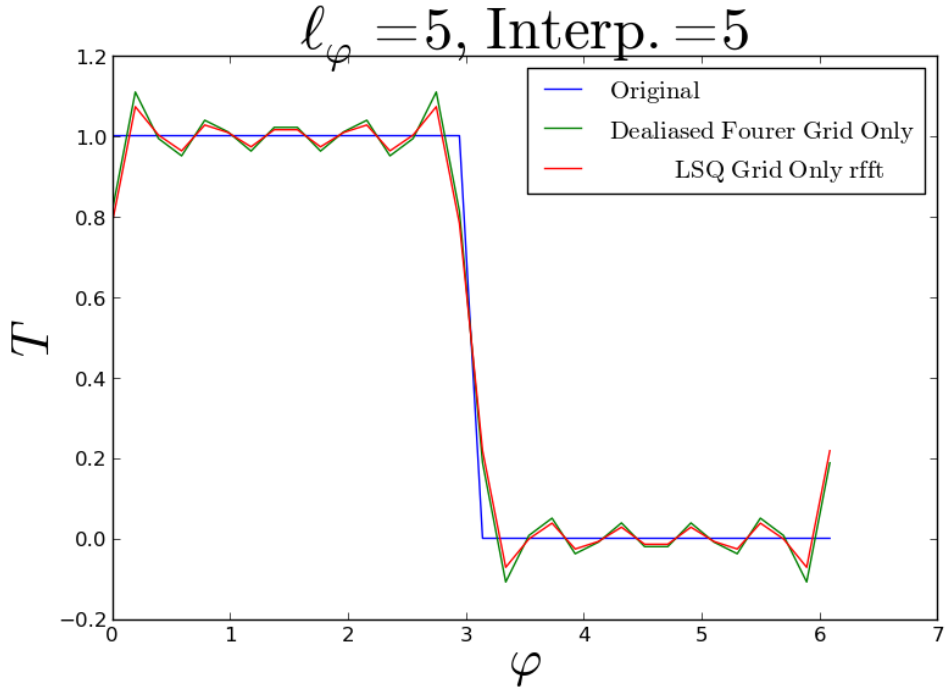

Another method used to try to improve NIMROD's capabilities with toroidal variation is matrix preconditioning.

- With fine toroidal resolution, solving the algebraic system for the implicit **B** advance is the limiting computational issue.
- Similar to previous work, we couple the resistivity Fourier components in the preconditioned matrix.[6]
- This couples off-diagonal components for the magnetic field advance. So far, an off-diagonal coupling of ± 1 has been used.

[6] Sovinec, NIMROD Team Meeting 2008-08, Fourier-off-diagonal preconditioning...

The resistivity preconditioning follows Hall MHD, but without hall terms.

- The resistivity and current density need to be convoluted. First resistivity, which is stored on the toroidal grid is put into it's Fourier form.
- We use that

$$\eta(\phi) = \sum_{j_1} \alpha_{j_1} \eta_{j_1} e^{ij_1\phi}$$

$$\mathbf{J}(\phi) = \sum_{l} \sum_{j} \alpha_{jl} J_{jl} e^{ij\phi}$$

$$\mathbf{A}(\phi) = \sum_{l} \sum_{j} \alpha_{jl} e^{ij\phi}$$

where $\alpha_{jl} = \alpha_j \hat{\mathbf{e}}_l$ where $\hat{\mathbf{e}}_l$ ranges over three basis vectors. So then, when we take parts of the sum $\eta\mathbf{J}$ for the preconditioning one must be careful about the subscript j (or j_1).

An example for the resistivity preconditioner.

- We have terms that looks like

$$(\boldsymbol{\nabla} \times \mathbf{A}^*) \cdot (\eta \mathbf{J})$$
$$(\boldsymbol{\nabla} \times \mathbf{A}^*) \cdot (\eta \frac{\boldsymbol{\nabla} \times \mathbf{B}}{\mu_0})$$

  where $\mathbf{A}$ is one of three basis function vectors.
- the $\eta \boldsymbol{\nabla} \times \mathbf{B}$ will be decomposed into basis functions $\mathbf{A}$, and so if we choose $\mathbf{A}_3^*$ and $\mathbf{A}_2$ we would have for the integrand that the component would be

$$\frac{\partial \alpha}{\partial z} \left(-\frac{\eta i k_{\text{col}}}{R} \alpha \right)$$

- If we choose $\mathbf{A}_2^*$ and $\mathbf{A}_2$ we would get

$$\frac{ik}{R} \alpha \left(-\frac{\eta i k_{\text{col}} \alpha}{R} \right) + \frac{\partial \alpha}{\partial r} \left(\eta \frac{\partial \alpha}{\partial r} \right)$$

Matrix preconditioning has not completely solved the problem.

- Matrix preconditioning has proven to be more efficient, but more sensitive to time-step size. It also has not improved performance during the non-linear phase when there is a large distortion away from axisymmetry.
- The divergence **B** cleaning appears to have a significant effect on the capability of the solver to go farther in time.
- The div-B diffusion constant can change the condition number. A large coefficient causes the time step to decrease. This points to the main problem for solving farther in time being in the magnetic field advance.

◊ Conclusions and Discussion

- External kinks can be simulated in NIMROD.
- Various measures to improve the robustness of the external kink simulation have been considered.
- To successfully simulate external kinks, improving the 3D preconditioning is needed.

Future Work

- Improving 3D preconditioning.
- Simulate external kinks further in time in both cylindrical and toroidal geometries.
- Calculate forces and thermal loads on the device due to VDE and external kinks.
- Evolve more nonlinear cases with realistic and relevant geometries.